Black Carbon Involved Photochemistry Enhances the Formation of Sulfate in the Ambient Atmosphere: Evidence from *in-situ* Individual Particle Investigation

Guohua Zhang[1,2,3,*], Yuzhen Fu[1,2,4], Xiaocong Peng[1,2,4], Wei Sun[1,2,4], Zongbo Shi[5], Wei Song[1,2,3], Weiwei Hu[1,2,3], Duohong Chen[6], Xiufeng Lian[7], Lei Li[7], Mingjin Tang[1,2,3], Xinming Wang[1,2,3], Xinhui Bi[1,2,3,*]

[1] State Key Laboratory of Organic Geochemistry and Guangdong Provincial Key Laboratory of Environmental Protection and Resources Utilization, Guangzhou Institute of Geochemistry, Chinese Academy of Sciences (CAS), Guangzhou 510640, PR China

[2] CAS Center for Excellence in Deep Earth Science, Guangzhou, 510640, China

[3] Guangdong-Hong Kong-Macao Joint Laboratory for Environmental Pollution and Control, Guangzhou Institute of Geochemistry, CAS, Guangzhou 510640, PR China

[4] University of Chinese Academy of Sciences, Beijing 100049, PR China

[5] School of Geography, Earth and Environmental Sciences, University of Birmingham, Birmingham B15 2TT, U.K.

[6] State Environmental Protection Key Laboratory of Regional Air Quality Monitoring, Guangdong Environmental Monitoring Center, Guangzhou 510308, PR China

[7] Institute of Mass Spectrometer and Atmospheric Environment, Jinan University, Guangzhou 510632, PR China

*Corresponding to Guohua Zhang (zhanggh@gig.ac.cn) and Xinhui Bi (bixh@gig.ac.cn)

Abstract

Mixing state of black carbon (BC) with secondary species has been highlighted as a major uncertainty in assessing its radiative forcing. While recent laboratory simulation has demonstrated that BC could serve as a catalyst to enhance the formation of sulfate, its role in the formation and evolution of secondary aerosols in the real atmosphere remains poorly understood. In the present study, the mixing of BC with sulfate/nitrate in the atmosphere of Guangzhou (China) was directly investigated with a single particle aerosol mass spectrometer (SPAMS). The peak area ratios of sulfate to nitrate (SNRs) for the BC-containing particles are constantly higher than those of the BC-free particles (defined as particles with negligible BC signals). Furthermore, the seasonal SNR peak is observed in summer and autumn, and the diurnal peak is found in the afternoon, consistent with the trends of radiation-related parameters (i.e., solar radiation and temperature), pointing to the BC-induced photochemical production of sulfate. Such hypothesis is further supported by the multilinear regression and random forest analysis, showing that the variation of SNRs associated with the BC-containing particles could be well explained (R^2 = ~0.7-0.8) by the radiation-related parameters (> 30% of the variance) and the relative BC content (~20%) in individual particles, but with limited influence of precursors (SO_2/NO_x: < 5%). Differently, the radiation-related factors only explain < 10% of the SNR variation for the BC-free particles. These results provide ambient observational evidence pointing to a unique role of BC on the photochemical formation and evolution of sulfate, which merits further quantitative evaluations.

Keywords: black carbon; sulfate; individual particles; mixing state; SPAMS

Key points:

1. Enhanced sulfate to nitrate ratios (SNRs) are observed for the BC-containing particles

2. The distinct diurnal variation of the enhanced SNRs is most likely attributed to BC catalytic photochemistry

3. SNRs in individual BC-containing particles could be well predicted by the radiation-related parameters and the relative BC content

1 Introduction

As a substantial fraction of atmospheric aerosols, black carbon (BC) or soot enhances haze pollution, modifies the regional meteorology, and imposes a tremendous positive forcing on the global climate by absorbing solar radiation [*Bond et al.*, 2013; *Ding et al.*, 2016; *Penner*, 2019]. While freshly emitted BC contains limited coating, atmospheric aging such as coagulation with other particles, condensation of vapors, and cloud processing will lead to internally mixed BC particles with complex compositions [*Zhang et al.*, 2018; *Riemer et al.*, 2019]. These aging processes result in considerable variability in morphology, mixing state, and hygroscopic and optical properties of BC particles, subsequently leading to the modification of climatic and health effects [*Zhang et al.*, 2008; *He et al.*, 2015; *Peng et al.*, 2016]. Nevertheless, significant discrepancies between standard model predictions and regionally-specific observations are tightly related to distinct compositional heterogeneity (or mixing state) among BC particles [*Liu et al.*, 2017; *Matsui et al.*, 2018; *Fierce et al.*, 2020].

As one of the most critical factors determining the absorption of BC, the mixing state of individual BC particles is highly complicated and constantly changing during their transport in the atmosphere. BC particles were observed to be extensively internally mixed worldwide [*Adachi et al.*, 2016; *Liu et al.*, 2017; *Zhang et al.*, 2017; *Motos et al.*, 2019], including various areas around China, such as the Pearl River Delta (PRD) region [*Huang et al.*, 2012; *Zhang et al.*, 2014; *Tan et al.*, 2016], Yangtze River Delta region [*Kleffmann and Wiesen*, 2005], and North China Plain [*Cheng et al.*, 2009; *Zhang et al.*, 2018; *Yu et al.*, 2020], leading to significantly enhanced light scattering and absorption capacity of BC. While extensive studies

have gained insight into the evolution of mixing state of BC particles, it has been merely linked to the condensation of secondary species, such as sulfate, nitrate, and organics [*Cahill et al.*, 2012; *Zhang et al.*, 2013; *Zhang et al.*, 2018; *Yuan et al.*, 2019]. Actually, BC can be actively involved in the formation of secondary species, through interacting with atmospheric reactive species, such as NO_2, SO_2, O_3, and HNO_3 [*Kleffmann and Wiesen*, 2005; *McCabe and Abbatt*, 2009; *Khalizov et al.*, 2010; *Han et al.*, 2013b; *Zhao et al.*, 2017]. A recent laboratory study indicates that the BC catalytic chemistry should play a considerable role in the enhanced sulfate formation during the regional haze in China, in the presence of ammonia and NO_2 [*Zhang et al.*, 2020]. Besides, the photochemical oxidation of some intrinsic organic compositions by O_2 might also be an essential aging process for BC [*Han et al.*, 2012]. There is also growing evidence demonstrating that BC is photoactive and could release reactive oxygen species (ROS) including $^1O_2$ and ·OH, which may represent a crucial aging pathway of BC [*Gehling and Dellinger*, 2013; *Li et al.*, 2018b; *Li et al.*, 2019].

Despite environmental significance, whether the intrinsic properties of BC particles are significant in the formation and evolution of secondary compositions in the ambient atmosphere remains poorly understood. The main challenge to address such issues in field measurement is to track the heterogeneous reactions unique to the BC-containing particles, which relies on individual particle techniques accompanied with chemical information. For instance, with an Aerodyne soot particle - aerosol mass spectrometer (SP-AMS), various non-refractory species (e.g., sulfate, nitrate, and organics) associated with refractory BC can be quantitatively traced in real-time [*Lee et al.*, 2015; *Wang et al.*, 2016b]. The temporal variation of secondary

compositions internally mixed with BC could also be indicated by single-particle mass spectrometry (SPMS), despite only semi-quantitative information obtained [*Cahill et al.*, 2012; *Healy et al.*, 2012; *Zhang et al.*, 2014]. Measurements with both techniques have indicated that active photochemical formation of oxidized organics and sulfate could lead to a distinct diurnal circle of mixing state of BC-containing particles. However, the role of BC in such chemistry has not been identified yet. In addition, there is still a lack of treatments for heterogeneous reactions on different types of particles in most models [*Zheng et al.*, 2015]. Therefore, it is necessary to comprehensively evaluate the effect of heterogeneous chemistry involving BC particles on the formation of secondary compositions.

In the present study, a Single Particle Aerosol Mass Spectrometer (SPAMS) was applied to measure the size and chemical compositions of individual particles, in order to accommodate the specific role of BC in the formation of secondary species. The variation of sulfate (with nitrate as a reference) associated with both the BC-containing and BC-free particles, and also their diurnal trends, are analyzed and discussed. The main objectives are (1) to verify whether BC regulates the formation and evolution of sulfate in the ambient atmosphere and (2) to explore the dependence of sulfate production on atmospheric conditions, including their precursors and meteorological parameters.

2 Methods

2.1 Data collection

On-line measurements were conducted at a representative urban site in Guangzhou (China) [*Zhang et al.*, 2019a], a megacity in the PRD region. The measurements cover four seasons,

including spring (21/02 to 11/04, 2014), summer (13/06 to 16/07, 2013), autumn (26/09 to 19/10, 2013), and winter (15/12 to 25/12, 2013). The sampling inlet for fine particle characterization was situated ~40 meters above the ground level.

The size and chemical composition of dried individual particles were obtained by the SPAMS (Hexin Analytical Instrument Co., Ltd., China) in real-time [*Li et al.*, 2011]. Briefly, particles are introduced into the SPAMS through a critical orifice. They are focused and accelerated to specific velocities determined by two diode Nd:YAG laser beams (532 nm) located 6 cm apart. Based on the measured velocities, a pulsed laser (266 nm) downstream can be triggered to desorb/ionize these individual particles, and ion fragments were produced and measured by a time-of-flight mass spectrometer. As a result, velocity, detection moment, and mass spectrum for each ionized particle are recorded. The velocity could be converted to vacuum aerodynamic diameter (d_{va}) based on a calibration function created using polystyrene latex spheres (PSL, Duke Scientific Corp., Palo Alto) with predefined sizes.

The auxiliary meteorological data, including ambient temperature (T), relative humidity (RH) and wind speed (WS), and concentration of gaseous pollutants (SO_2, NO_x, and O_3), BC, and $PM_{2.5}$, provided by Guangdong Environmental Monitoring Center, are shown as diurnal trends in Fig. S1 (Supporting Information).

2.2 Data analysis

2.2.1 SPAMS Data

BC-containing particles are classified according to the relative peak area (RPA) of carbon ion cluster (i.e., m/z ±12[C].$^{+/-}$, ±36[C_3].$^{+/-}$, ±48[C_4].$^{+/-}$ or ±60[C_5].$^{+/-}$), which is set as larger

than 0.05. And thus, particles with RPA < 0.05 are regarded as BC-free particles. The potential influence of the arbitrarily defined RPA for BC screening on the conclusions is also evaluated in section 3.4. Defined as the peak area of each m/z divided by the total ion mass spectral peak areas, RPA is generally applied to indicate the relative fraction of a single species in individual particles [*Gross et al.*, 2000]. The BC-containing particles ruled out with such criteria account for ~60-80% of all the measured particles (Table S1), which are in the range of those reported in the urban atmosphere [*Healy et al.*, 2013].

The majority of the measured BC-containing particles distribute in a size range of 0.2–1.0 μm (Fig. S2a), generally consistent with their dominant mass fraction in the atmosphere of the PRD region [*Huang et al.*, 2012]. Representative ion peaks for the BC-containing particles, as presented in Fig. S2b, are carbon ion cluster (e.g., m/z $\pm12[C]^{+/-}$, $\pm36[C_3]^{+/-}$, $\pm48[C_4]^{+/-}$ and $\pm60[C_5]^{+/-}$), organic carbon (OC) fragments (m/z $27[C_2H_3]^+$, $29[C_2H_5]^+$, $37[C_3H]^+$, $26[CN]^-$, $42[CNO]^-$, and $43[C_2H_3O]^+$), and secondary inorganic species, such as sulfate ($-97[HSO_4]^-$), nitrate ($-62[NO_3]^-$), and ammonium ($18[NH_4]^+$). There are also some metallic species such as $23[Na]^+$ and $39[K]^+$.

In the present study, we mainly focus on the difference of sulfate to nitrate ratio (SNR) between the BC-containing and BC-free particles. The respective RPA ratios of sulfate and nitrate between the BC-containing and BC-free particles were compared over the seasons, as shown in Fig. S3. These ratios show significant variations, with higher values for sulfate RPA ratios and lower values for nitrate RPA ratios in the BC-containing particles, indicating a relatively higher fraction of sulfate rather than nitrate in these particles. It is also noted that the

sulfate RPAs are lower for the BC-containing particles than the BC-free particles, which is likely attributable to the matrix effect during the ionization. And thus, only the SNR is applied to make it comparable between the BC-containing and BC-free particles.

2.2.2 Multiple linear and random forest regression

Multiple linear and random forest analysis, explicitly describing a relationship between predictor and response variables (i.e., regressors) [*Berk*, 2008], are applied to estimate the relative contribution of several factors to the variations of SNRs for the BC-containing and BC-free particles, respectively. In the multiple linear models, the least-squares fit is used, and two of the most common measures of model fit are the residual standard error and the proportion of variance explained (R^2). Furthermore, the Relaimpo package is used to assess the relative importance of regressors in the linear model and offers the possibility of bootstrapping them [*Groemping*, 2006]. Differently, random forest is for nonlinear multiple regression and has been widely applied for prediction and classification, using trees as building blocks to construct powerful prediction models [*Breiman*, 2001]. The algorithm first creates multiple decision trees, where each tree is grown by using the bootstrap re-sampling method. The relative importance of the predictor variables can also be obtained, with “Mean Decrease Accuracy” presenting the capability of each independent variable in explaining the variability of SNRs.

3 Results and Discussion

3.1 Distinct variations of SNR associated with the BC-containing particles

As can be seen in Fig. 1, the variations of SNR are distinguished between the BC-containing and BC-free particles. The SNR shows an apparent seasonal variation, with higher

values in summer and autumn but lower in spring and winter. Despite the similar SNR variations for both particle types over the seasons, the SNRs in the BC-containing particles are obviously higher than those in the BC-free particles. In particular, the average SNR for the BC-containing particles is ~2 times those for the BC-free particles in summer and autumn. Such a seasonal variation of SNR is similar to the concentration ratio observed for fine particles in Beijing, with the mean SNR in warmer seasons more than two times in cold seasons [*Li et al.*, 2020]. However, the difference of SNRs between the BC-containing and BC-free particles cannot be ruled out based on previous bulk analysis.

There is a pronounced diurnal variation of SNRs for the BC-containing particles over the seasons (Fig. 1b). A sharp increase of the SNRs in the BC-containing particles, rather than the BC-free particles, started at noon hour (~12:00). On the other hand, the SNRs of the BC-containing particles decreased from the highest values during the afternoon hours to the lowest contribution during nighttime or early morning. The diurnal trend of SNRs for the BC-containing particles is generally similar to that of temperature (Fig. S4). In both the BC-containing and BC-free particles, nitrate varied in a similar trend, decreasing during the afternoon but increasing during nighttime (Fig. 2), most probably attributed to the heterogeneous uptake of N_2O_5 onto the wet aerosols during high the RH period [*Lee et al.*, 2003; *Wang et al.*, 2009]. The different SNR trends between the BC-containing and BC-free particles could be mainly attributed to the increase of sulfate RPA during the afternoon, specific for the BC-containing particles. Sulfate associated with the BC-free particles does not show a clear trend, but with a distinct afternoon peak in the BC-containing particles (Fig. 2). And thus, the

198 diurnal variation of SNR is most probably driven by the variation of nitrate in the BC-free
199 particles.

200 The diurnal variation of SNRs and BC mixing state is generally consistent with the
201 previously reported data. Distinct diurnal cycles of secondary compositions associated with
202 BC-containing particles in Yangtze River Delta, China [*Wang et al.*, 2016b; *Li et al.*, 2018a],
203 with the increase of sulfate and low volatile oxidized organics in the afternoon due to
204 photochemical oxidation; however, with nitrate peaking during nighttime, driven by
205 thermodynamic equilibria and gas-to-particle partitioning [*Wang et al.*, 2016b]. There are also
206 several studies reporting a correlation between the fraction of internally mixed BC and
207 photochemical activities [*Wang et al.*, 2017; *Xu et al.*, 2018], mainly attributed to the
208 condensation of secondarily formed compositions. Photochemical processing of fresh fractal
209 BC emitted in the early morning to develop a highly aged one, internally mixed with OC,
210 ammonium, sulfate, and nitrate in the afternoon, has been directly observed in Mexico City
211 [*Moffet and Prather*, 2009]. Fast coating of BC was typically found during noontime
212 corresponding to high photochemistry intense and oxidants levels [*Zhang et al.*, 2018; *Liu et*
213 *al.*, 2020]. However, the behavior of BC-free particles has not been reported yet, hindering a
214 further understanding of BC's role in the diurnal variation of SNRs or mixing state.

215 **3.2 Most possible mechanism for the BC-enhanced SNRs**

216 Overall, we found that the SNR for the BC-containing particles is significantly higher than
217 that for the BC-free particles, reflecting a distinct behavior of BC-containing particles towards
218 the formation and evolution of sulfate. The diurnal trend of nitrate and sulfate associated with

both the BC-containing and BC-free particles, as discussed above, further indicates that it is the enhanced photochemical formation of sulfate on the BC-containing particles that leads to the higher SNRs. It is the heterogeneous processes that are important since the condensation of gaseous sulfuric and nitric acid gases is expected to be similar for different kinds of particles. The first evidence is the consistent trends between the seasonal and diurnal trends of the SNRs (Fig. 1) and temperature (Fig. S4), which implies a substantial role of photochemistry in the evolution of the BC-containing particles. Compared with the BC-free particles, the role of such chemistry involving BC is evident with a distinctly higher SNR peak in the afternoon hours. In contrast, it seems that the variations of SNRs cannot be simply explained by atmospheric oxidants ($O_x = O_3 + NO_x$) and the trend of their precursors SO_2/NO_x ($R^2 = 0.05$, $p < 0.01$) (Figs. S1 and S3). The second evidence comes from that the increase of SNRs towards higher relative BC content (Fig. S5), indicating that the BC fraction increase might contribute to additional oxidants. The relative importance of these factors, including radiation-related parameters (i.e., solar radiation and temperature) and the relative BC content in individual particles, in the variation of SNRs for the BC-containing particles, as discussed in section 3.3, further supports the significance of BC-induced photochemistry. As demonstrated by laboratory results, elemental carbon in BC-containing particles can act as a photoactive substrate and has notable catalytic effects on reactions through electronic transfer in the presence of O_2, which produces additional ROS, including $^1O_2$ and ·OH [*Li et al.*, 2018b; *Li et al.*, 2019; *Zhu et al.*, 2020]. Furthermore, there are also studies reporting the direct contribution of the additional ROS to the formation of sulfate from the oxidation of SO_2 on the surface of BC particles [*Novakov et*

240 *al.*, 1974; *Zhao et al.*, 2017]. And the production could be significantly enhanced with the
241 coexistence of O_3 [*Xu et al.*, 2015; *He et al.*, 2017]. However, the interactions between BC
242 particles and NO_2 unlikely to contribute to the formation of nitrate [*Han et al.*, 2013a; *Guan et*
243 *al.*, 2017].

244 There are also some possible explanations against the above hypothesis but are unlikely to
245 be significant. One is that BC and sulfate or their precursors originate from the same primary
246 sources. This seems unlikely given a relatively low correlation ($R^2 = 0.26$, $p < 0.01$) between
247 the temporal diurnal profiles of the concentration of BC and SO_2. BC is generally produced by
248 incomplete combustion, whereas sulfate is most probably from the secondary process involving
249 the oxidation of its precursor SO_2 [*Xiao et al.*, 2009; *Xue et al.*, 2019], which could be co-
250 emitted with BC. BC is most attributable to the traffic emission in the studied region, with a
251 higher correlation with NO_x ($R^2 = 0.63$, $p < 0.01$), whereas SO_2 or sulfate is mainly produced
252 by coal combustion or biomass burning [*Wang et al.*, 2016c]. Secondly, one may expect that
253 BC facilitates the depletion of nitrate, including evaporation and photochemical degradation.
254 While the additional heat due to the light-absorbing nature of BC may enhance the evaporation
255 of nitrate, our data show that such an effect is limited (Figs. 2 and S4). Although photochemical
256 degradation of nitrate may improve the heterogeneous oxidation of SO_2 through the produced
257 in-particle oxidants (OH, NO_2, and NO_2^-/HNO_2) [*Gen et al.*, 2019; *Zhang et al.*, 2019b], there
258 is still no evidence showing the influence of BC in the photochemistry of nitrate (Fig. S3).
259 Thirdly, higher SNRs associated with BC may also be explained by the fact the freshly emitted
260 smaller BC particles facilitate the condensation of H_2SO_4, due to their larger surface area

concentration. However, as shown in Fig. S2, the majority of the BC-containing particles were located in the size range of 0.2-1.0 μm, and extensively mixed with secondary components, which could be regarded as aged particles. More directly, the SNRs show no clear trend with increasing size (Fig. S6), further suggesting the limited influence of particle size on the variation of SNRs.

In addition, the role of the transition metals, such as Fe and V, that catalyzed the formation of sulfate [*Ault et al.*, 2010; *Zhang et al.*, 2019a] could be negligible due to their limited number fraction (< 3% on average) and no preferential association with the BC-containing particles. It is also possible that other oxidants (e.g., organic radicals, H_2O_2) play an indispensable role in the evolution of sulfate, yet it is beyond the scope of the present study.

3.3 Factors determining the variations of SNRs

To elucidate the relative importance of various meteorological and chemical factors on the variation of SNRs, multilinear regression is applied to include the most possible influencing factors, i.e., T, RH, O_x, solar radiation (SR), and SO_2/NO_x [*Xu et al.*, 2015; *He et al.*, 2017; *Wang et al.*, 2019a], on the variations of SNRs during the daytime, when the SR data are available. An additional factor, i.e., the relative BC fraction, is added to the regression for the BC-containing particles. As shown in Fig. 3, SNRs in both the BC-containing and BC-free particles could be well explained by these factors, with the evaluation of the model performance provided in Fig. S7. Notably, the variation of the SNRs for the BC-containing particles can be better predicted ($R^2 = 0.68$, $p < 0.01$) by these variables than that for the BC-free particles ($R^2 = 0.40$, $p < 0.01$). The addition of the relative BC fraction in the regression improves the

correlation coefficient R^2 from 0.54 to 0.68 for the BC-containing particles. An estimation of the relative importance of the predictors shows that the SNRs for the BC-containing particles are mainly dependent on the T (27%), RH (17%), and relative BC content (13%), but with limit dependence on the SO_2/NO_x (2%). Differently, the SNRs for the BC-free particles are dominantly determined by RH (19%), with modest contribution from SO_2/NO_x (7%), O_x (7%), and T (5%).

Consistently, random forest analysis could predict ~80% of the SNR variation for the BC-containing particles, and the most important three predictors are T (26%), relative BC content (25%), and RH (17%), as shown in Fig. S8. Since the diurnal variation of T typically tracks the strength of photochemistry [*He et al.*, 2011; *Xu et al.*, 2017], such results further support the importance of photochemistry and the relative BC content in the evolution of sulfate associated with BC. While the analysis may not reliably inform the complex chemical mechanisms of BC involved production of sulfate, the well-fitted results could still indicate the significance of various factors in the variation of SNRs.

3.4 Limitations

The main limitation or bias in the present study is the use of RPA in these qualitative individual mass spectral data rather than the absolute mass concentrations for individual species. It should be noted that it is still quite challenging for the SPAMS based on laser-ablation to provide quantitative information for individual species, due to various uncertainties induced by the laser ionization, such as matrix effects and incomplete ionization [*Jeong et al.*, 2011; *Healy et al.*, 2013; *Zhou et al.*, 2016]. Despite this, the variation of RPA is still a good indicator for

303 the investigation of atmospheric processing and mixing state of various particle types, including
304 BC-containing particles, at an individual particle level [*Wang et al.*, 2010; *Zauscher et al.*, 2013;
305 *Zhang et al.*, 2014]. In the present study, even though it is insufficient to provide a quantitative
306 assessment of SNRs on the BC-containing particles, our results do successfully identify a
307 distinct behavior of BC-containing particles in the ambient atmosphere and thus have an
308 advantage of providing a qualitative or semi-quantitative understanding of the evolution of
309 SNRs associated with BC. Future work should target a quantitative understanding of the
310 laboratory kinetics of the photochemical reactions of BC-containing particles, e.g., with
311 Aerodyne SP-AMS.

312 Another limitation is related to identifying the individual BC-containing particles based
313 on the arbitrary defined RPA of carbon ion clusters (i.e., > 0.05). However, as can be seen in
314 Fig. S6, the average SNRs generally increase towards higher relative BC content, regardless of
315 the deviation. It indicates that the methodology for the identification of the BC-containing
316 particles would not lead to an ambiguous conclusion on the distinct behavior of the BC-
317 containing and BC-free particles. While some particle types, including pure ammonium sulfate,
318 and certain organic, cannot simply be ionized by SPAMS, the measured BC-free particles
319 should be still representative of the majority of particle types observed in the urban atmosphere.
320 As shown by microscopic analysis, such pure compounds limitedly contribute to the particle
321 population in a typical urban atmosphere [*Fu et al.*, 2012; *Li et al.*, 2016].

322 **4 Conclusions and Implications**

Our results provide observational evidence, extending the laboratory results to the ambient atmosphere that BC could act as a photoactive and absorbing substrate [*Li et al.*, 2018b; *Li et al.*, 2019], leading to an enrichment of sulfate. Since there is considerable debate regarding the mechanism for SO_2 oxidation [*Wang et al.*, 2016a; *Xue et al.*, 2016; *Gen et al.*, 2019; *Wang et al.*, 2019b; *Wang et al.*, 2020a; *Wang et al.*, 2020c], our finding further underscores the importance of the intrinsic property of BC on the photochemical evolution of sulfate, in particular, during summer and autumn. Given that BC accounts for an essential part of particles in the urban atmosphere [*Ding et al.*, 2016; *Tan et al.*, 2016; *Wang et al.*, 2020b], such a role might be critical for the formation and evolution of sulfate. *Liu et al.* [2019a] observed increasing SNR with altitude over Beijing and attributed the vertical profile to various factors, including plenary boundary layer structure, regional transportation, emission variation, and the aging process of aerosols and gaseous precursors during vertical diffusion. Our analysis may provide an additional explanation associated with photochemistry on the BC-containing particles. The mechanism might also be particularly important during haze episodes when heterogeneous chemistry is thought to play a considerable role in sulfate production [*Zheng et al.*, 2015; *Li et al.*, 2020].

A most recent chamber simulation reveals that efficient sulfate formation from BC catalyzed SO_2 oxidation in the presence of NO_2 and NH_3 under dark conditions [*Zhang et al.*, 2020]. Our evidence further suggests that the photochemical activities during the daytime might also be significant for the production of sulfate and influencing the evolution of BC in the atmosphere. Regarding that sulfate is one of the primary drivers of the BC absorption

enhancement in the severely polluted areas in China [*Chen et al.*, 2017], the relative enrichment of sulfate on BC may also partly explain the substantial diurnal variability of light absorption enhancement and single-scattering albedo for BC in eastern China [*Xu et al.*, 2018]. However, the influence of BC on the formation of secondary compositions is rarely considered in models [*Matsui*, 2016], although it is well-known that accounting for variability in per-particle composition and properties would help improve absorption enhancement predictions [*Fierce et al.*, 2020]. Therefore, to account for the evolution and climate impact of BC accurately, it is essential to include BC involved photochemistry in the regional aerosol-climate modeling, since the associated sulfate are critical to evaluate the hygroscopic, phase, and optical properties of BC-containing particles [*Ramana et al.*, 2010; *Sun et al.*, 2018; *Liu et al.*, 2019b].

Acknowledgments

This work was funded by the National Natural Science Foundation of China (42077322, 41775124, and 41877307), Natural Science Foundation of Guangdong Province (2019B151502022), Youth Innovation Promotion Association CAS (2021354), and Guangdong Foundation for Program of Science and Technology Research (2019B121205006 and 2020B1212060053).

Conflict of Interest

There are no conflicts of interest in the article.

Data Availability Statement

The processed data supporting this paper are available on Zenodo (10.5281/zenodo.4650206).

References

Adachi, K., N. Moteki, Y. Kondo, and Y. Igarashi (2016), Mixing states of light-absorbing particles measured using a transmission electron microscope and a single-particle soot photometer in Tokyo, Japan, *J. Geophys. Res.-Atmos.*, *121*(15), 2016JD025153, doi:10.1002/2016JD025153.

Ault, A. P., C. J. Gaston, Y. Wang, G. Dominguez, M. H. Thiemens, and K. A. Prather (2010), Characterization of the Single Particle Mixing State of Individual Ship Plume Events Measured at the Port of Los Angeles, *Environ. Sci. Technol.*, *44*(6), 1954-1961, doi:10.1021/es902985h.

Berk, R. A. (2008), Random Forests, in *Statistical Learning from a Regression Perspective*, edited, pp. 1-63, Springer New York, New York, NY, doi:10.1007/978-0-387-77501-2_5.

Bond, T. C., et al. (2013), Bounding the role of black carbon in the climate system: A scientific assessment, *J. Geophys. Res.-Atmos.*, *118*(11), 5380-5552, doi:10.1002/Jgrd.50171.

Breiman, L. (2001), Random Forests, *Mach. Learn.*, *45*(1), 5-32, doi:10.1023/A:1010933404324.

Cahill, J. F., K. Suski, J. H. Seinfeld, R. A. Zaveri, and K. A. Prather (2012), The mixing state of carbonaceous aerosol particles in northern and southern California measured during CARES and CalNex 2010, *Atmos. Chem. Phys.*, *12*(22), 10989-11002, doi:10.5194/acp-12-10989-2012.

Chen, B., Z. Zhu, X. Wang, A. Andersson, J. Chen, Q. Zhang, and Ö. Gustafsson (2017), Reconciling modeling with observations of radiative absorption of black carbon aerosols, *J. Geophys. Res.-Atmos.*, *122*(11), 5932-5942, doi:10.1002/2017JD026548.

Cheng, Y. F., et al. (2009), Influence of soot mixing state on aerosol light absorption and single scattering albedo during air mass aging at a polluted regional site in northeastern China, *J. Geophys. Res.-Atmos.*, *114*(D2), D00G10, doi:10.1029/2008jd010883.

Ding, A. J., et al. (2016), Enhanced haze pollution by black carbon in megacities in China, *Geophys. Res. Lett.*, *43*(6), 2873-2879, doi:10.1002/2016GL067745.

Fierce, L., et al. (2020), Radiative absorption enhancements by black carbon controlled by particle-to-particle heterogeneity in composition, *Proc. Natl. Acad. Sci. USA*, *117*(10), 5196-5203, doi:10.1073/pnas.1919723117 %J

Fu, H., M. Zhang, W. Li, J. Chen, L. Wang, X. Quan, and W. Wang (2012), Morphology, composition and mixing state of individual carbonaceous aerosol in urban Shanghai, *Atmos. Chem. Phys.*, *12*(2), 693-707, doi:10.5194/acp-12-693-2012.

Gehling, W., and B. Dellinger (2013), Environmentally Persistent Free Radicals and Their Lifetimes in PM2.5, *Environ. Sci. Technol.*, *47*(15), 8172-8178, doi:10.1021/es401767m.

Gen, M., R. Zhang, D. D. Huang, Y. Li, and C. K. Chan (2019), Heterogeneous SO2 Oxidation in Sulfate Formation by Photolysis of Particulate Nitrate, *Environ. Sci. Tech. Let.*, *6*(2), 86-91, doi:10.1021/acs.estlett.8b00681.

Groemping, U. (2006), Relative Importance for Linear Regression in R: The Package relaimpo, *J. Stat. Softw.*, *17*(1), 1-27, doi:10.18637/jss.v017.i01.

Gross, D. S., M. E. Galli, P. J. Silva, and K. A. Prather (2000), Relative sensitivity factors for alkali metal and ammonium cations in single particle aerosol time-of-flight mass spectra, *Anal. Chem.*, *72*(2), 416-422.

Guan, C., X. Li, W. Zhang, and Z. Huang (2017), Identification of Nitration Products during Heterogeneous Reaction of NO2 on Soot in the Dark and under Simulated Sunlight, *J. Phys. Chem. A*, *121*(2), 482-492, doi:10.1021/acs.jpca.6b08982.

Han, C., Y. Liu, and H. He (2013a), Heterogeneous photochemical aging of soot by NO2 under simulated sunlight, *Atmos. Environ.*, *64*, 270-276, doi:10.1016/j.atmosenv.2012.10.008.

Han, C., Y. Liu, and H. He (2013b), Role of Organic Carbon in Heterogeneous Reaction of NO2 with Soot, *Environ. Sci. Technol.*, *47*(7), 3174-3181, doi:10.1021/es304468n.

Han, C., Y. C. Liu, J. Z. Ma, and H. He (2012), Key role of organic carbon in the sunlight-enhanced atmospheric aging of soot by O-2, *Proc. Natl. Acad. Sci. USA*, *109*(52), 21250-21255, doi:10.1073/pnas.1212690110.

He, C., K. N. Liou, Y. Takano, R. Zhang, M. L. Zamora, P. Yang, Q. Li, and L. R. Leung (2015), Variation of the radiative properties during black carbon aging: theoretical and experimental intercomparison, *Atmos. Chem. Phys.*, *15*(20), 11967-11980, doi:10.5194/acp-15-11967-2015.

He, L. Y., X. F. Huang, L. Xue, M. Hu, Y. Lin, J. Zheng, R. Y. Zhang, and Y. H. Zhang (2011), Submicron aerosol analysis and organic source apportionment in an urban atmosphere in Pearl River Delta of China using high-resolution aerosol mass spectrometry, *J. Geophys. Res.-Atmos.*, *116*(D12304), 1-15, doi:10.1029/2010jd014566.

He, X., S. Pang, J. Ma, and Y. Zhang (2017), Influence of relative humidity on heterogeneous reactions of 03 and O-3/SO2 with soot particles: Potential for environmental and health effects, *Atmos. Environ.*, *165*, 198-206, doi:10.1016/j.atmosenv.2017.06.049.

Healy, R. M., et al. (2013), Quantitative determination of carbonaceous particle mixing state in Paris using single-particle mass spectrometer and aerosol mass spectrometer measurements, *Atmos. Chem. Phys.*, *13*(18), 9479-9496, doi:10.5194/acp-13-9479-2013.

Healy, R. M., et al. (2012), Sources and mixing state of size-resolved elemental carbon particles in a European megacity: Paris, *Atmos. Chem. Phys.*, *12*(4), 1681-1700, doi:10.5194/acp-12-1681-2012.

Huang, X. F., T. L. Sun, L. W. Zeng, G. H. Yu, and S. J. Luan (2012), Black carbon aerosol characterization in a coastal city in South China using a single particle soot photometer, *Atmos. Environ.*, *51*, 21-28, doi:10.1016/j.atmosenv.2012.01.056.

Jeong, C. H., M. L. McGuire, K. J. Godri, J. G. Slowik, P. J. G. Rehbein, and G. J. Evans (2011), Quantification of aerosol chemical composition using continuous single particle measurements, *Atmos. Chem. Phys.*, *11*(14), 7027-7044, doi:10.5194/acp-11-7027-2011.

Khalizov, A. F., M. Cruz-Quinones, and R. Y. Zhang (2010), Heterogeneous Reaction of NO2 on Fresh and Coated Soot Surfaces, *J. Phys. Chem. A*, *114*(28), 7516-7524, doi:10.1021/jp1021938.

Kleffmann, J., and P. Wiesen (2005), Heterogeneous conversion of NO2 and NO on HNO3 treated soot surfaces: atmospheric implications, *Atmos. Chem. Phys.*, *5*, 77-83, doi:10.5194/acp-5-77-2005.

Lee, A. K. Y., M. D. Willis, R. M. Healy, T. B. Onasch, and J. P. D. Abbatt (2015), Mixing state of carbonaceous aerosol in an urban environment: single particle characterization using the soot particle aerosol mass spectrometer (SP-AMS), *Atmos. Chem. Phys.*, *15*(4), 1823-1841, doi:10.5194/acp-15-1823-2015.

Lee, S. H., D. M. Murphy, D. S. Thomson, and A. M. Middlebrook (2003), Nitrate and oxidized organic ions in single particle mass spectra during the 1999 Atlanta Supersite Project, *J. Geophys. Res.*, *108*(D7), 8417, doi:10.1029/2001jd001455.

Li, K. N., X. N. Ye, H. W. Pang, X. H. Lu, H. Chen, X. F. Wang, X. Yang, J. M. Chen, and Y. J. Chen (2018a), Temporal variations in the hygroscopicity and mixing state of black carbon aerosols in a polluted megacity area, *Atmos. Chem. Phys.*, *18*(20), 15201-15218, doi:10.5194/acp-18-15201-2018.

Li, L., et al. (2011), Real time bipolar time-of-flight mass spectrometer for analyzing single aerosol particles, *Intl. J. Mass. Spectrom.*, *303*(2-3), 118-124, doi:10.1016/j.ijms.2011.01.017.

Li, M., F. Bao, Y. Zhang, H. Sheng, C. Chen, and J. Zhao (2019), Photochemical Aging of Soot in the Aqueous Phase: Release of Dissolved Black Carbon and the Formation of 1O2, *Environ. Sci. Technol.*, *53*(21), 12311-12319, doi:10.1021/acs.est.9b02773.

Li, M., F. Bao, Y. Zhang, W. Song, C. Chen, and J. Zhao (2018b), Role of elemental carbon in the photochemical aging of soot, *Proc. Natl. Acad. Sci. USA*, *115*(30), 7717-7722, doi:10.1073/pnas.1804481115.

Li, S., et al. (2020), Characterizing the ratio of nitrate to sulfate in ambient fine particles of urban Beijing during 2018–2019, *Atmos. Environ.*, 117662, doi:https://doi.org/10.1016/j.atmosenv.2020.117662.

Li, W. J., L. Y. Shao, D. Z. Zhang, C. U. Ro, M. Hu, X. H. Bi, H. Geng, A. Matsuki, H. Y. Niu, and J. M. Chen (2016), A review of single aerosol particle studies in the atmosphere of East Asia: morphology, mixing state, source, and heterogeneous reactions, *J. Clean. Prod.*, *112*, 1330-1349, doi:10.1016/j.jclepro.2015.04.050.

Liu, D. T., et al. (2017), Black-carbon absorption enhancement in the atmosphere determined by particle mixing state, *Nature Geosci.*, *10*(3), 184-U132, doi:10.1038/Ngeo2901.

Liu, H., X. L. Pan, D. T. Liu, X. Y. Liu, X. S. Chen, Y. Tian, Y. L. Sun, P. Q. Fu, and Z. F. Wang (2020), Mixing characteristics of refractory black carbon aerosols at an urban site in Beijing, *Atmos. Chem. Phys.*, *20*(9), 5771-5785, doi:10.5194/acp-20-5771-2020.

Liu, Q., J. Quan, X. Jia, Z. Sun, X. Li, Y. Gao, and Y. Liu (2019a), Vertical Profiles of Aerosol Composition over Beijing, China: Analysis of In Situ Aircraft Measurements, *J. Atmos. Sci.*, *76*(1), 231-245, doi:10.1175/JAS-D-18-0157.1 %J Journal of the Atmospheric Sciences.

Liu, Y., Z. Wu, X. Huang, H. Shen, Y. Bai, K. Qiao, X. Meng, W. Hu, M. Tang, and L. He (2019b), Aerosol Phase State and Its Link to Chemical Composition and Liquid Water Content in a Subtropical Coastal Megacity, *Environ. Sci. Technol.*, *53*(9), 5027-5033, doi:10.1021/acs.est.9b01196.

Matsui, H. (2016), Black carbon simulations using a size- and mixing-state-resolved three-dimensional model: 1. Radiative effects and their uncertainties, *J. Geophys. Res.-Atmos.*, *121*(4), 1793-1807, doi:10.1002/2015jd023998.

Matsui, H., D. S. Hamilton, and N. M. Mahowald (2018), Black carbon radiative effects highly sensitive to emitted particle size when resolving mixing-state diversity, *Nat. Commun.*, *9*, doi:10.1038/s41467-018-05635-1.

McCabe, J., and J. P. D. Abbatt (2009), Heterogeneous Loss of Gas-Phase Ozone on n-Hexane Soot Surfaces: Similar Kinetics to Loss on Other Chemically Unsaturated Solid Surfaces, *J. Phys. Chem. C*, *113*(6), 2120-2127, doi:10.1021/jp806771q.

Moffet, R. C., and K. A. Prather (2009), In-situ measurements of the mixing state and optical properties of soot with implications for radiative forcing estimates, *Proc. Natl. Acad. Sci. USA*, *106*(29), 11872-11877, doi:10.1073/pnas.0900040106.

Motos, G., J. Schmale, J. C. Corbin, M. Zanatta, U. Baltensperger, and M. Gysel-Beer (2019), Droplet activation behaviour of atmospheric black carbon particles in fog as a function of their size and mixing state, *Atmos. Chem. Phys.*, *19*(4), 2183-2207, doi:10.5194/acp-19-2183-2019.

Novakov, T., S. G. Chang, and A. B. Harker (1974), Sulfates as Pollution Particulates: Catalytic Formation on Carbon (Soot) Particles, *Science*, *186*(4160), 259, doi:10.1126/science.186.4160.259.

Peng, J. F., et al. (2016), Markedly enhanced absorption and direct radiative forcing of black carbon under polluted urban environments, *Proc. Natl. Acad. Sci. USA*, *113*(16), 4266-4271, doi:10.1073/pnas.1602310113.

Penner, J. E. (2019), Soot, sulfate, dust and the climate - three ways through the fog, *Nature*, *570*(7760), 158-159, doi:10.1038/d41586-019-01791-6.

Ramana, M. V., V. Ramanathan, Y. Feng, S. C. Yoon, S. W. Kim, G. R. Carmichael, and J. J. Schauer (2010), Warming influenced by the ratio of black carbon to sulphate and the black-carbon source, *Nature Geosci.*, *3*(8), 542-545, doi:10.1038/Ngeo918.

Riemer, N., A. P. Ault, M. West, R. L. Craig, and J. H. Curtis (2019), Aerosol Mixing State: Measurements, Modeling, and Impacts, *Rev. Geophys.*, *57*(2), 187-249, doi:10.1029/2018rg000615.

Sun, J. X., et al. (2018), Key Role of Nitrate in Phase Transitions of Urban Particles: Implications of Important Reactive Surfaces for Secondary Aerosol Formation, *J. Geophys. Res.-Atmos.*, *123*(2), 1234-1243, doi:10.1002/2017JD027264.

Tan, H. B., L. Liu, S. J. Fan, F. Li, Y. Yin, M. F. Cai, and P. W. Chan (2016), Aerosol optical properties and mixing state of black carbon in the Pearl River Delta, China, *Atmos. Environ.*, *131*, 196-208, doi:10.1016/j.atmosenv.2016.02.003.

Wang, G., et al. (2016a), Persistent sulfate formation from London Fog to Chinese haze, *Proc. Natl. Acad. Sci. USA*, *113*(48), 13630, doi:10.1073/pnas.1616540113.

Wang, H., et al. (2019a), Aerosols in an arid environment: The role of aerosol water content, particulate acidity, precursors, and relative humidity on secondary inorganic aerosols, *Sci. Total. Environ.*, *646*, 564-572, doi:https://doi.org/10.1016/j.scitotenv.2018.07.321.

Wang, J., et al. (2020a), Fast sulfate formation from oxidation of SO2 by NO2 and HONO observed in Beijing haze, *Nat. Commun.*, *11*(1), 2844, doi:10.1038/s41467-020-16683-x.

Wang, J., et al. (2017), First Chemical Characterization of Refractory Black Carbon Aerosols and Associated Coatings over the Tibetan Plateau (4730 m a.s.l), *Environ. Sci. Technol.*, *51*(24), 14072-14082, doi:10.1021/acs.est.7b03973.

Wang, J. F., X. L. Ge, Y. F. Chen, Y. F. Shen, Q. Zhang, Y. L. Sun, J. Z. Xu, S. Ge, H. Yu, and M. D. Chen (2016b), Highly time-resolved urban aerosol characteristics during springtime in Yangtze River Delta, China: insights from soot particle aerosol mass spectrometry, *Atmos. Chem. Phys.*, *16*(14), 9109-9127, doi:10.5194/acp-16-9109-2016.

538 Wang, Q., et al. (2020b), Measurement report: Source and mixing state of black carbon
539 aerosol in the North China Plain: implications for radiative effect, *Atmos. Chem. Phys.*, *20*(23),
540 15427-15442, doi:10.5194/acp-20-15427-2020.
541 Wang, Q. Y., et al. (2016c), Physicochemical characteristics of black carbon aerosol and
542 its radiative impact in a polluted urban area of China, *J. Geophys. Res.-Atmos.*, *121*(20), 12505-
543 12519, doi:10.1002/2016jd024748.
544 Wang, S., S. Zhou, Y. Tao, W. G. Tsui, J. Ye, J. Z. Yu, J. G. Murphy, V. F. McNeill, J. P.
545 D. Abbatt, and A. W. H. Chan (2019b), Organic Peroxides and Sulfur Dioxide in Aerosol:
546 Source of Particulate Sulfate, *Environ. Sci. Technol.*, doi:10.1021/acs.est.9b02591.
547 Wang, X., et al. (2020c), Atmospheric Photosensitization: A New Pathway for Sulfate
548 Formation, *Environ. Sci. Technol.*, doi:10.1021/acs.est.9b06347.
549 Wang, X. F., S. Gao, X. Yang, H. Chen, J. M. Chen, G. S. Zhuang, J. D. Surratt, M. N.
550 Chan, and J. H. Seinfeld (2010), Evidence for High Molecular Weight Nitrogen-Containing
551 Organic Salts in Urban Aerosols, *Environ. Sci. Technol.*, *44*(12), 4441-4446.
552 Wang, X. F., Y. P. Zhang, H. Chen, X. Yang, J. M. Chen, and F. H. Geng (2009),
553 Particulate Nitrate Formation in a Highly Polluted Urban Area: A Case Study by Single-Particle
554 Mass Spectrometry in Shanghai, *Environ. Sci. Technol.*, *43*(9), 3061-3066,
555 doi:10.1021/es8020155.
556 Xiao, R., et al. (2009), Formation of submicron sulfate and organic aerosols in the outflow
557 from the urban region of the Pearl River Delta in China, *Atmos. Environ.*, *43*(24), 3754-3763.
558 Xu, W., et al. (2017), Effects of Aqueous-Phase and Photochemical Processing on
559 Secondary Organic Aerosol Formation and Evolution in Beijing, China, *Environ. Sci. Technol.*,
560 *51*(2), 762-770, doi:10.1021/acs.est.6b04498.
561 Xu, W., Q. Li, J. Shang, J. Liu, X. Feng, and T. Zhu (2015), Heterogeneous oxidation of
562 SO2 by O3-aged black carbon and its dithiothreitol oxidative potential, *J. Environ. Sci.*, *36*, 56-
563 62, doi:https://doi.org/10.1016/j.jes.2015.02.014.

Xu, X. Z., et al. (2018), The influence of photochemical aging on light absorption of atmospheric black carbon and aerosol single-scattering albedo, *Atmos. Chem. Phys.*, *18*(23), 16829-16844, doi:10.5194/acp-18-16829-2018.

Xue, J., X. Yu, Z. Yuan, S. M. Griffith, A. K. H. Lau, J. H. Seinfeld, and J. Z. Yu (2019), Efficient control of atmospheric sulfate production based on three formation regimes, *Nature Geosci.*, *12*(12), 977-982, doi:10.1038/s41561-019-0485-5.

Xue, J., Z. Yuan, S. M. Griffith, X. Yu, A. K. H. Lau, and J. Z. Yu (2016), Sulfate Formation Enhanced by a Cocktail of High NOx, SO2, Particulate Matter, and Droplet pH during Haze-Fog Events in Megacities in China: An Observation-Based Modeling Investigation, *Environ. Sci. Technol.*, *50*(14), 7325-7334, doi:10.1021/acs.est.6b00768.

Yu, C. J., D. T. Liu, K. Broda, R. Joshi, J. Olfert, Y. L. Sun, P. Q. Fu, H. Coe, and J. D. Allan (2020), Characterising mass-resolved mixing state of black carbon in Beijing using a morphology-independent measurement method, *Atmos. Chem. Phys.*, *20*(6), 3645-3661, doi:10.5194/acp-20-3645-2020.

Yuan, Q., J. Xu, Y. Wang, X. Zhang, Y. Pang, L. Liu, L. Bi, S. Kang, and W. Li (2019), Mixing State and Fractal Dimension of Soot Particles at a Remote Site in the Southeastern Tibetan Plateau, *Environ. Sci. Technol.*, *53*(14), 8227-8234, doi:10.1021/acs.est.9b01917.

Zauscher, M. D., Y. Wang, M. J. K. Moore, C. J. Gaston, and K. A. Prather (2013), Air Quality Impact and Physicochemical Aging of Biomass Burning Aerosols during the 2007 San Diego Wildfires, *Environ. Sci. Technol.*, *47*(14), 7633-7643, doi:10.1021/es4004137.

Zhang, F., et al. (2020), An unexpected catalyst dominates formation and radiative forcing of regional haze, *Proc. Natl. Acad. Sci. USA*, *117*(8), 3960-3966, doi:10.1073/pnas.1919343117.

Zhang, G., et al. (2017), The single-particle mixing state and cloud scavenging of black carbon: a case study at a high-altitude mountain site in southern China, *Atmos. Chem. Phys.*, *17*(24), 14975-14985, doi:10.5194/acp-17-14975-2017.

Zhang, G., et al. (2019a), Oxalate Formation Enhanced by Fe-Containing Particles and Environmental Implications, *Environ. Sci. Technol.*, *53*(3), 1269-1277, doi:10.1021/acs.est.8b05280.

592 Zhang, G. H., X. H. Bi, J. J. He, D. H. Chen, L. Y. Chan, G. W. Xie, X. M. Wang, G. Y.
593 Sheng, J. M. Fu, and Z. Zhou (2014), Variation of secondary coatings associated with elemental
594 carbon by single particle analysis, *Atmos. Environ.*, *92*, 162-170,
595 doi:10.1016/j.atmosenv.2014.04.018.
596 Zhang, G. H., X. H. Bi, L. Li, L. Y. Chan, M. Li, X. M. Wang, G. Y. Sheng, J. M. Fu, and
597 Z. Zhou (2013), Mixing state of individual submicron carbon-containing particles during spring
598 and fall seasons in urban Guangzhou, China: a case study, *Atmos. Chem. Phys.*, *13*(9), 4723-
599 4735, doi:10.5194/acp-13-4723-2013.
600 Zhang, R. Y., A. F. Khalizov, J. Pagels, D. Zhang, H. X. Xue, and P. H. McMurry (2008),
601 Variability in morphology, hygroscopicity, and optical properties of soot aerosols during
602 atmospheric processing, *Proc. Natl. Acad. Sci. USA*, *105*(30), 10291-10296,
603 doi:10.1073/pnas.0804860105.
604 Zhang, Y., F. Bao, M. Li, C. Chen, and J. Zhao (2019b), Nitrate-Enhanced Oxidation of
605 SO2 on Mineral Dust: A Vital Role of a Proton, *Environ. Sci. Technol.*, *53*(17), 10139-10145,
606 doi:10.1021/acs.est.9b01921.
607 Zhang, Y., et al. (2018), Sizing of Ambient Particles From a Single-Particle Soot
608 Photometer Measurement to Retrieve Mixing State of Black Carbon at a Regional Site of the
609 North China Plain, *J. Geophys. Res.-Atmos.*, *123*(22), 12778-12795,
610 doi:10.1029/2018jd028810.
611 Zhao, Y., Y. Liu, J. Ma, Q. Ma, and H. He (2017), Heterogeneous reaction of SO2 with
612 soot: The roles of relative humidity and surface composition of soot in surface sulfate formation,
613 *Atmos. Environ.*, *152*, 465-476, doi:http://dx.doi.org/10.1016/j.atmosenv.2017.01.005.
614 Zheng, B., Q. Zhang, Y. Zhang, K. B. He, K. Wang, G. J. Zheng, F. K. Duan, Y. L. Ma,
615 and T. Kimoto (2015), Heterogeneous chemistry: a mechanism missing in current models to
616 explain secondary inorganic aerosol formation during the January 2013 haze episode in North
617 China, *Atmos. Chem. Phys.*, *15*(4), 2031-2049, doi:10.5194/acp-15-2031-2015.

618 Zhou, Y., et al. (2016), A field measurement based scaling approach for quantification of
619 major ions, organic carbon, and elemental carbon using a single particle aerosol mass
620 spectrometer, *Atmos. Environ.*, *143*, 300-312, doi:10.1016/j.atmosenv.2016.08.054.
621 Zhu, J., J. Shang, Y. Chen, Y. Kuang, and T. Zhu (2020), Reactive Oxygen Species-
622 Related Inside-to-Outside Oxidation of Soot Particles Triggered by Visible-Light Irradiation:
623 Physicochemical Property Changes and Oxidative Potential Enhancement, *Environ. Sci.*
624 *Technol.*, doi:10.1021/acs.est.0c01150.
625

626 **Figure Caption**

627 **Figure 1.** (a) Seasonal variation of SNRs for the BC-containing and BC-free particles,
628 respectively. Box and whisker plot shows lower, median, and upper lines, denoting
629 the 25th, 50th, and 75th percentiles, respectively; the lower and upper edges denote
630 the 10th and 90th percentiles, respectively. (b) Diurnal variation of SNRs for the BC-
631 containing and BC-free particles, respectively. The shadings indicate the 95%
632 confidence intervals of the hourly mean values.

633 **Figure 2.** The diurnal trends of sulfate and nitrate RPA in the (a) BC-containing and
634 (b) BC-free particles, respectively.

635 **Figure 3.** Comparison between the measured and regressed SNRs, and the relative
636 importance of various factors on the variations of SNRs for the (a and c) BC-
637 containing and (b and d) BC-free particles, respectively. The shadings for the
638 regressed line (a and b) indicate the 95% confidence intervals. The error bars (in c and
639 d) provide confidence intervals for the relative importance with 100 bootstrap
640 replicates to evaluate the results.
641

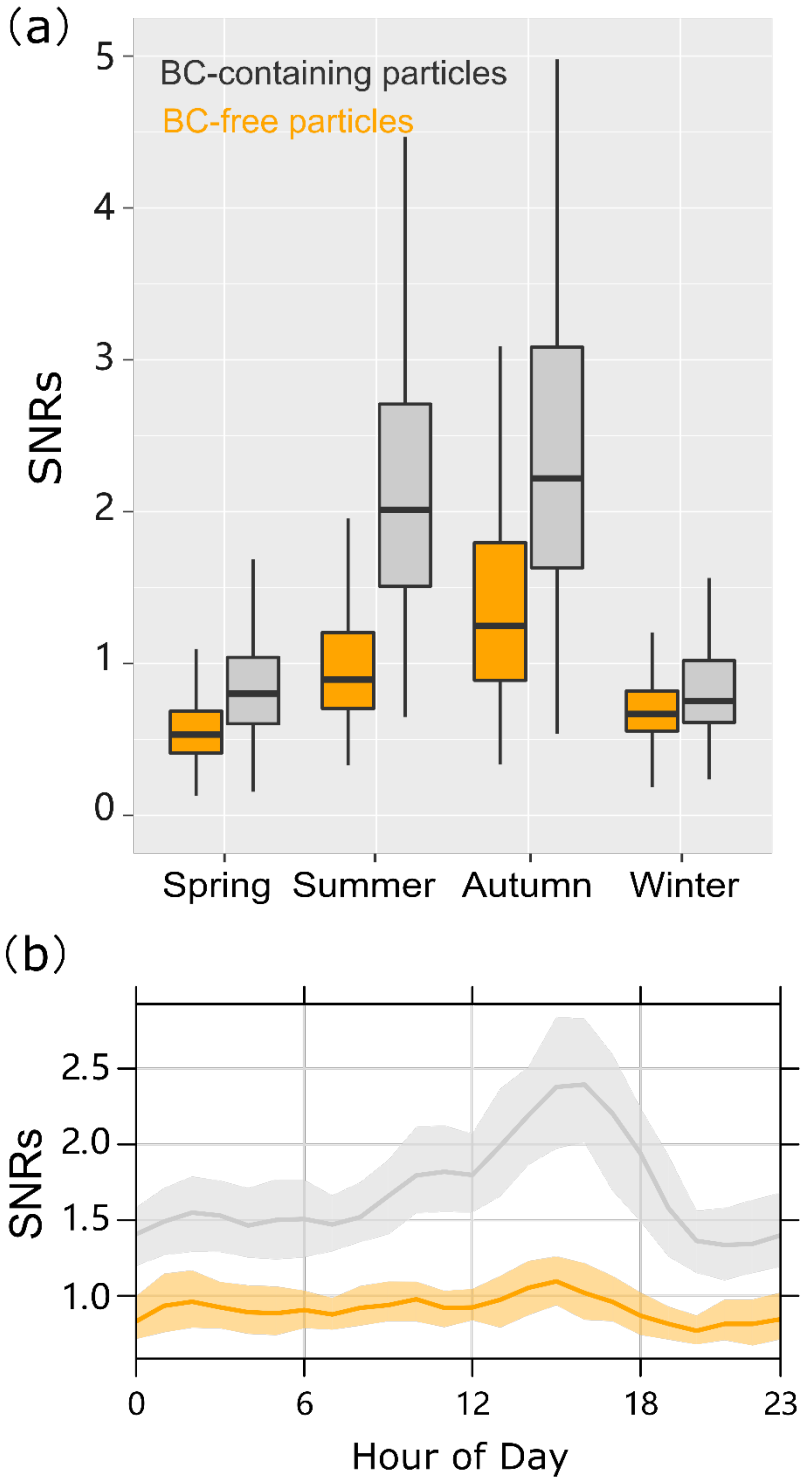
(a)
BC-containing particles
BC-free particles
SNRs
5
4
3
2
1
0
Spring
Summer
Autumn
Winter
(b)
SNRs
2.5
2.0
1.5
1.0
0
6
12
18
23
Hour of Day

642

643 **Fig. 1.**

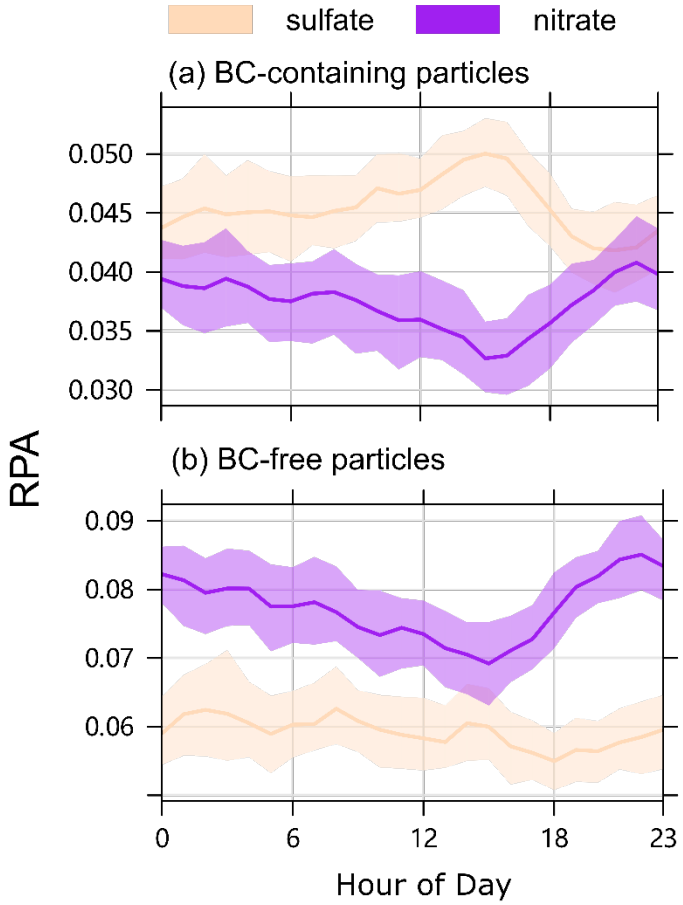
sulfate
nitrate
(a) BC-containing particles
0.050
0.045
0.040
0.035
0.030
RPA
(b) BC-free particles
0.09
0.08
0.07
0.06
0
6
12
18
23
Hour of Day

644

645 **Fig. 2.**

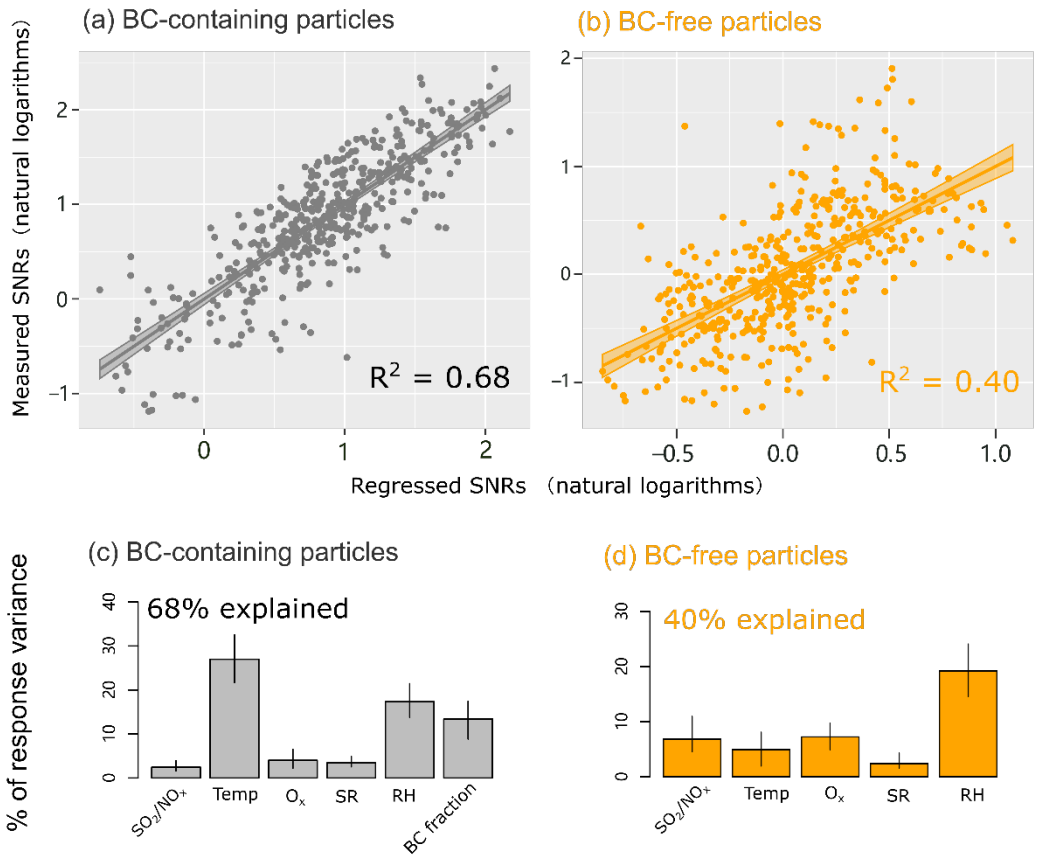
(a) BC-containing particles
(b) BC-free particles
Measured SNRs (natural logarithms)
Regressed SNRs (natural logarithms)
R2 = 0.68
R2 = 0.40
(c) BC-containing particles
(d) BC-free particles
% of response variance
68% explained
40% explained
SO2/NO+
Temp
Ox
SR
RH
BC fraction

646

647 Fig. 3.